Supplemental Material

for

"Capillary Thinning of Elastic and Viscoelastic Thread: from Elastocapillarity to Phase Separation"

H. V. M. Kibbelaar,[1] A. Deblais,[1,2] F. Burla,[3] G. H. Koenderink,[3,4] K. P. Velikov,[1,2] and D. Bonn[1]

[1]*Van der Waals-Zeeman Institute, Institute of Physics, University of Amsterdam, 1098 XH Amsterdam, The Netherlands.*

[2]*Unilever R&D Vlaardingen, Olivier van Noortlaan 120, 3133 AT Vlaardingen, The Netherlands.*

[3]*AMOLF, Department of Living Matter, 1098 XG Amsterdam, The Netherlands.*

[4]*Department of Bionanoscience, Kavli Institute of Nanoscience, Delft University of Technology, 2629 HZ Delft, The Netherlands.*

Abstract

This document provides supporting figures to accompany the main text; it gives more details on the experimental methods, the oscillatory shear measurements, the breakup dynamics of all the solutions at different pH, the shear and extensional rheology behaviour in Regime I, the break up dynamics of the fluid state and the extensional rates for both the 'fluid' and 'elastic' states extracted from the break up dynamics.

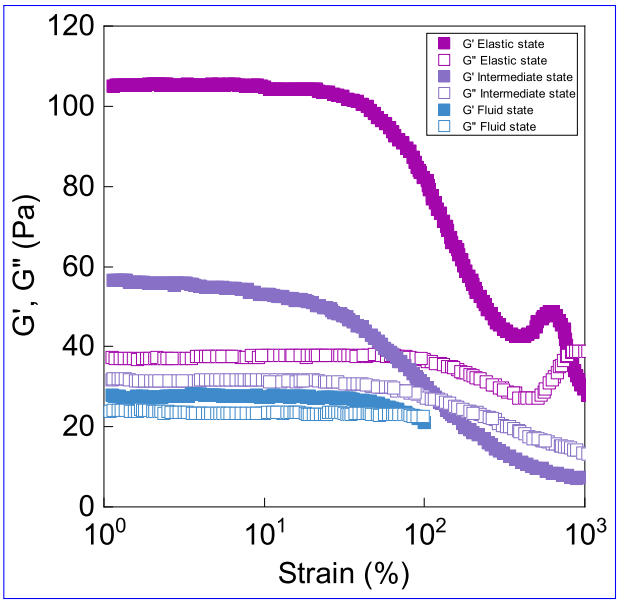

SUPPL. FIG. 1. Strain sweeps for the fluid state, intermediate state and elastic state. Further oscillatory shear measurements are well performed within the linear viscoelastic regime of HA.

I. Supplementary Note 1: Rheology measurements

Rheology measurements were performed with a stress-controlled rheometer (Anton Paar MCR 302), equipped with a cone plate geometry with a diameter of 50 mm and cone angle of 1°. The experiments were performed at a gap size of 52 μm and at a temperature of 22 °C set by a Peltier system. A humidity chamber around the geometry allow us to suppress evaporation during the whole measurement. Samples are left to equilibrate for 5 days to reach homogeneity and were loaded in the rheometer geometry using a spatula. After (thermal) equilibration measurements were performed. The elastic and viscous shear moduli were probed by performing oscillatory shear measurements at an oscillation frequency of 0.5 Hz and a strain amplitude of 0.5%, which is well within the linear viscoelastic regime for HA (see SUPPL. FIG.1.). The average reported is the representative of at least three independent measurements. The steady shear experiments were performed by carrying out a shear rate sweep from $1 \cdot 10^{-2}$ to 1000 s^{-1}. The flow curves were fitted to power law following $\sigma = K\dot{\gamma}^{\alpha}$, with K the flow consistency index. The reported results are averages of at least three measurements for each pH. For each sample, the pH was measured using a pH meter (Hanna Instruments).

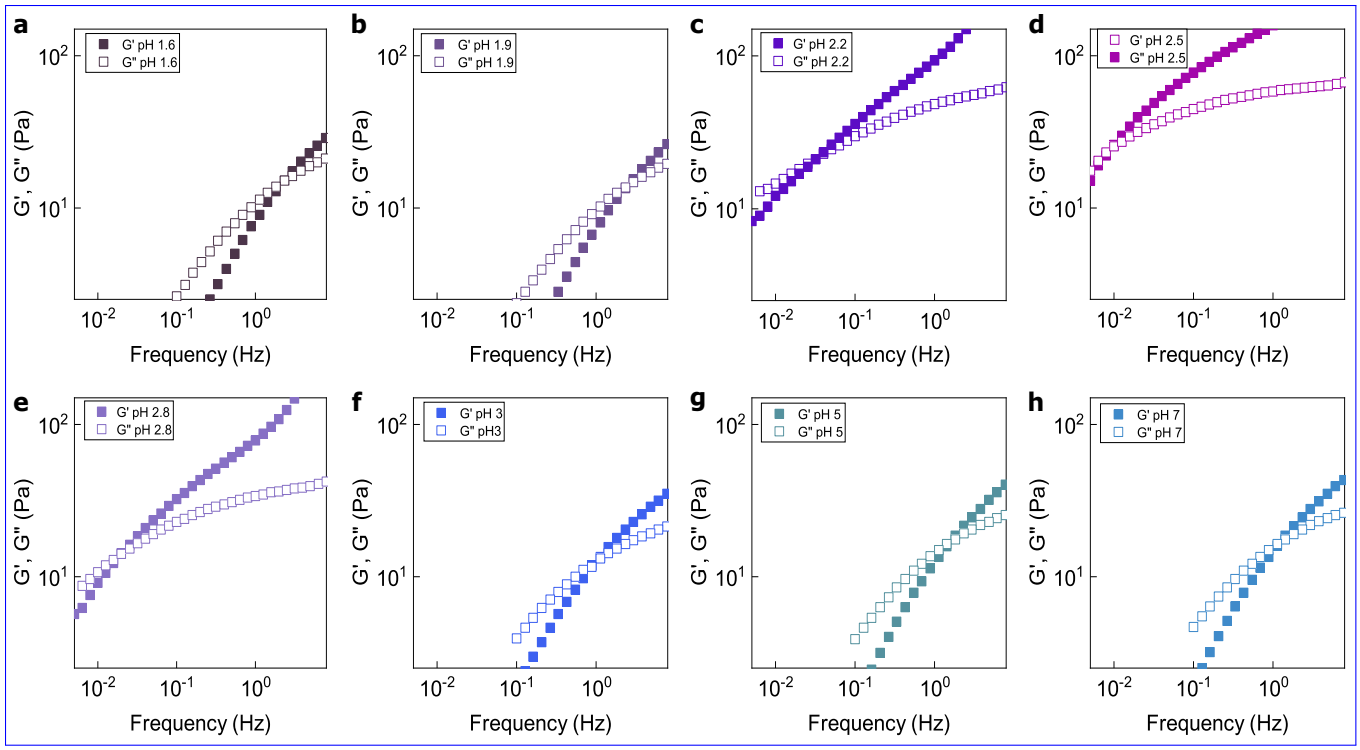

SUPPL. FIG. 2. (a-h) Oscillatory shear measurements of all pH, showing that the viscoelastic behaviour of HA strongly depends on the pH. The elastic and viscous moduli at f = 0.5 Hz and a strain amplitude of 0.5%. For the measurements at the pH of 2.2, 2.8 and 2.5, measurements needed to be performed at lower frequencies to observe the cross over point between G' and G".

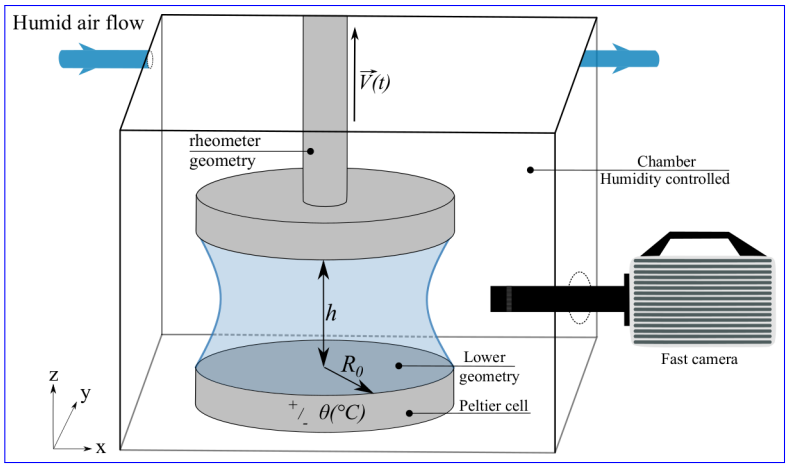

SUPPL. FIG. 3. Sketch of experimental set up (not to scale) to create a purely extensional flow to study the extensional thinning and destabilization of HA filaments. A rheometer (Anton paar, MCR 302) was used as the building block of the device. A rheometer geometry plate with a diameter of 5 mm was used, the lower plate having the same diameter. The upper plate can be pulled vertically at a constant velocity until the capillary bridge breaks. The Peltier cell allows us to impose the temperature of the sample during the elongational process at a constant speed. The evolution of the liquid bridge is recorded with a fast camera (Phantom V7) allowing frame rates up to 10.000 frames per second. The camera is equipped with a microscope tube lens, with an objective up to 12x magnification (Navitar) and a spatial resolution of 3 μm per pixel. The whole setup is placed in a chamber and is continuously flushed with humid air (80% RH) to prevent evaporation during the measurement.

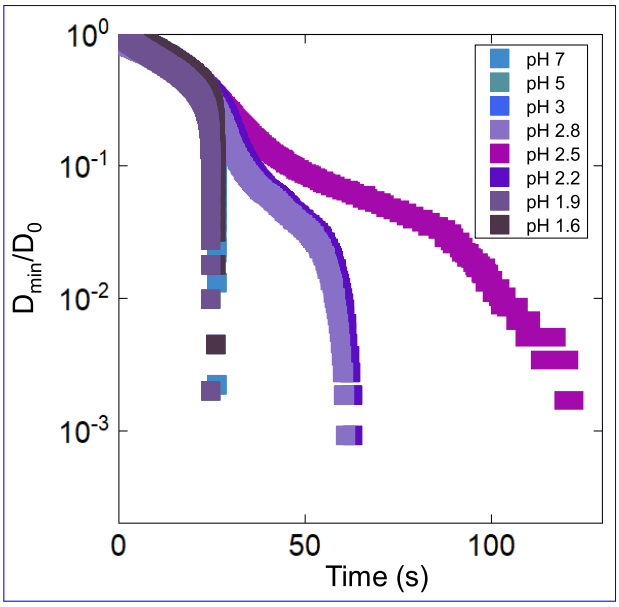

SUPPL. FIG. 4. Minimum filament diameter normalized by the initial bridge size for all pH. The dynamics of the solutions with pH 1.6, 1.9, 3, 5 and 7 are similar and there for categorized as 'fluid' state in the main text. The dynamics of of pH 2.2 and 2.8 are also similar and categorized as the 'intermediate' state. The solution at pH 2.5 shows the most elastic behaviour and is called the ' elastic' state.

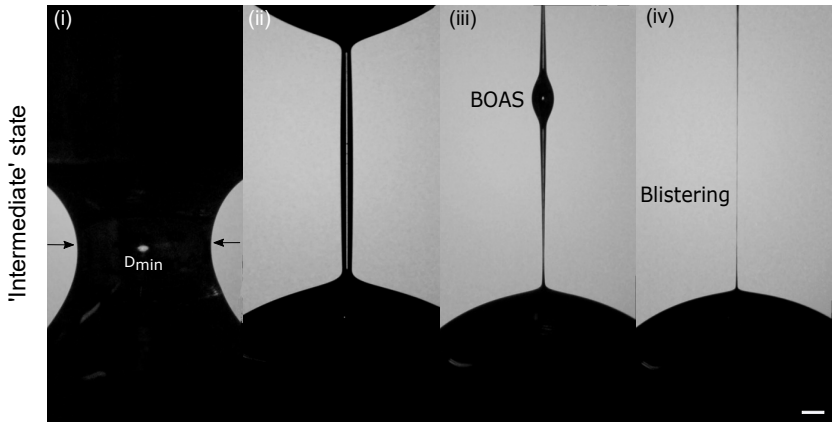

SUPPL. FIG. 5. Photographs of the breakup neck dynamics of the 'intermediate' state at pH 2.8. The numbers in the pictures correspond to the different regimes; (i) the power law fluid regime (I), (ii) the exponential thinning regime (II) where a slender filament and symmetry breaking occurs, (iii) and (iv) show the BOAS and blistering instabilities respectively, which occur in the regime where the extensional viscosity is saturated (III).

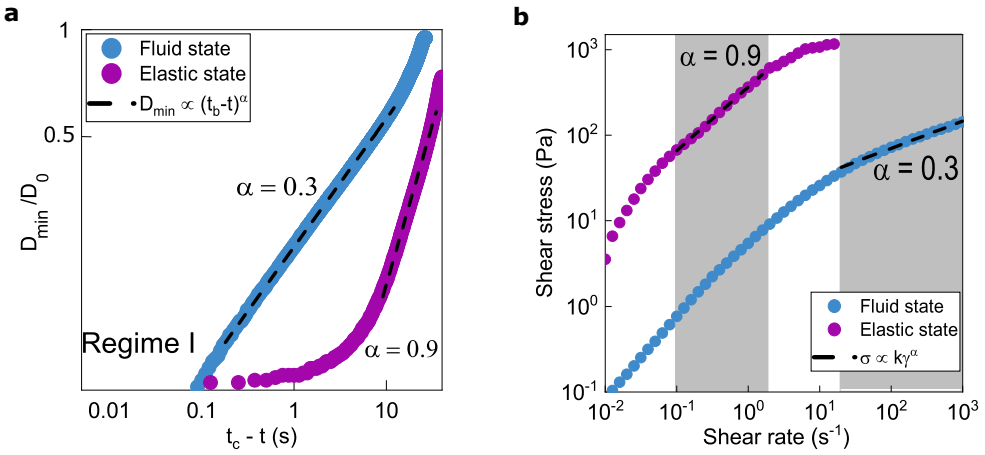

SUPPL. FIG. 6. (a) Normalized minimum neck diameter D_{min}/D_0 as a function of time $t_b - t$, where t_b is the breakup time. The first part of the breakup dynamics in Regime I (main text) is plotted. The neck thinning is similar to that of a power-law fluid. This regime (I) (see main text) follows $D_{min} = (t_b - t)^{\alpha}$, indicated by the black dashed fit, where α depends on the viscous or inviscid character of the fluid. The α values corresponding to the fluid and elastic state (blue and purple) are respectively 0.3 and 0.9. These power law exponents from the break up dynamics correspond to the power law exponents from the shear-thinning regime of the flow curve of the steady shear experiments (b) that follows $\sigma = K\dot{\gamma}^{\alpha}$, with K the flow consistency index. The grey coloured areas correspond to the fitted area in (a) and to the typical deformation rates of both solutions deduced from SUPPL. FIG. 3. (red)

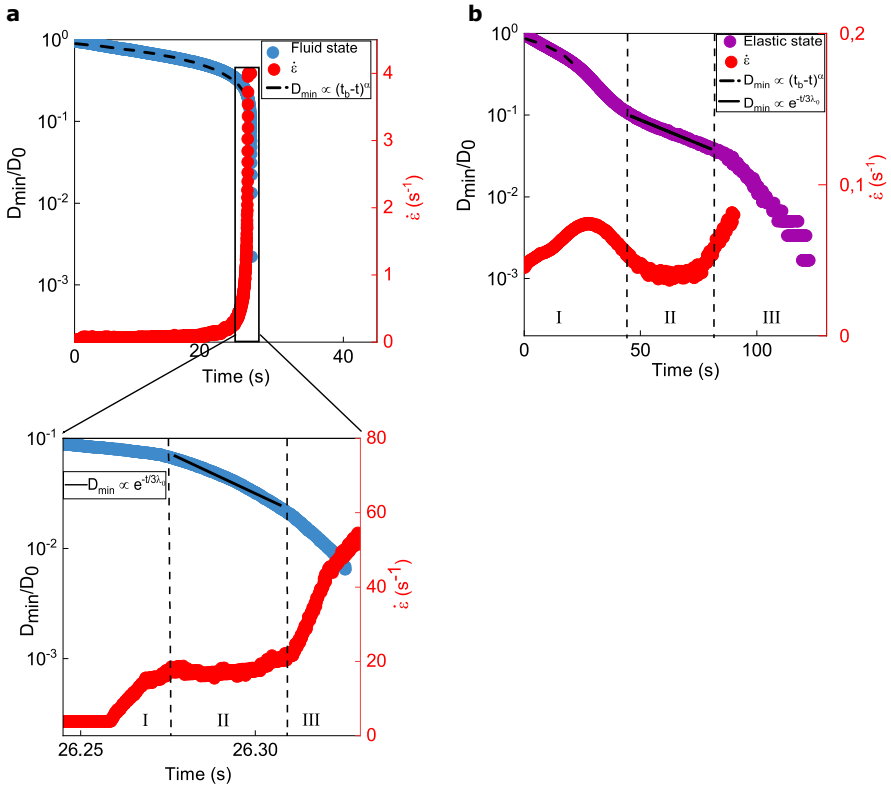

SUPPL. FIG. 7. Normalized minimum neck diameter D_{min}/D_0 and the corresponding extensional rates $\dot{\varepsilon}$ as a function of time for (a) the fluid state at pH 7 with an inset where the last part of the breakup can be observed in more detail and (b) the elastic state at pH 2.5. The extensional rate is directly obtained from the evolution of the filament diameter as $\dot{\varepsilon} = \frac{-2}{D_{min}} \frac{dD_{min}}{dt}$. From the extensional rate the different regimes can clearly be distinguished. The extensional rate increases as the neck diameter decreases corresponding to the powerlaw regime (I). Subsequently, the extensional rate is increasing and reaching a constant value where a long and slender filament is formed corresponding to the exponential thinning regime (II). After this regime, the extensional rate keeps increasing. This leads to an even steeper exponential decay (regime III) and eventually causing the breakup of the filament. Higher values of the extensional rate are found for the fluid state as this in agreement with smaller relaxation times (of milliseconds compared to seconds in the elastic state).

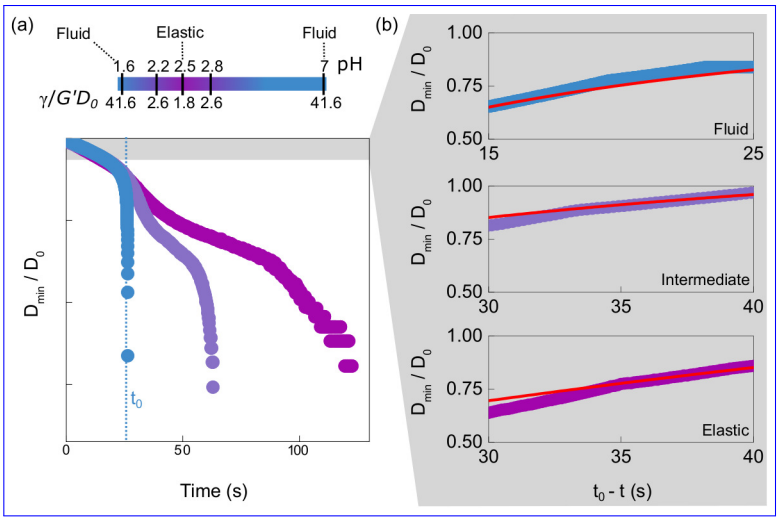

SUPPL. FIG. 8. (a) Minimum neck radius versus time in the different material state (different pH), where t_0 is the extrapolated time at which pinch off would take place without the visco-elasto-capillary regime. Same colored code as in the main text. (b) The red straight lines are exponential fits to the disturbance amplitude $1 - D_{min}/D_0$ in the very initial times of the thinning dynamics, from which we extracted the growth rates reported in Fig. 3 of the main text.